Manipulation of central amygdala neurotensin neurons alters alcohol consumption

María Luisa Torruella-Súarez[1,2], Jessica R. Vandenberg[2], Gregory J. Tipton[2], Brennon R. Luster[2,3], Kedar Dange[2], Gunjan K. Patel[2], Jenna A. McHenry[3,4], J. Andrew Hardaway[2,5], Pranish A. Kantak[3], Nicole A. Crowley[1,2], Jeffrey F. DiBerto[2, 5], Sara P. Faccidomo[2], Clyde W. Hodge[2,3], Garret D. Stuber[2,3,4], and Zoé A. McElligott[2,3,4,5,#]

1. Neuroscience Curriculum
2. Bowles Center for Alcohol Studies
3. Department of Psychiatry
4. Neuroscience Center
5. Department of Pharmacology

University of North Carolina at Chapel Hill, Chapel Hill, NC, USA, 27599

Corresponding author, zoemce@email.unc.edu

Abstract

The central nucleus of the amygdala plays a significant role in alcohol use and other affective disorders; however, the genetically-defined neuronal subtypes and their projections that govern these behaviors are not well known. Here we show that ablation of neurotensin-expressing neurons in the central nucleus of the amygdala of mice decreases their ethanol consumption and preference for ethanol. Furthermore, optogenetically stimulating projections from these neurons to the parabrachial nucleus is reinforcing, and increases ethanol consumption while reducing food consumption. These data suggest that this central amygdala to parabrachial nucleus projection influences the expression of reward-related phenotypes and is a novel circuit promoting alcohol consumption and regulating state-dependent food consumption.

Introduction

The central nucleus of the amygdala (CeA) is a heterogeneous structure that plays an important role in the regulation of appetitive, aversive, and ethanol-mediated behaviors (Mahler and Berridge, 2009; Tye *et al*, 2011; Robinson *et al*, 2014; McCall *et al*, 2015; Warlow *et al*, 2017; Kim *et al*, 2017; Douglass *et al*, 2017). While some data have shed light on the neuronal subpopulations influencing fear- and feeding-related behaviors (Haubensak *et al*, 2010; Cai *et al*, 2014; Douglass *et al*, 2017), it remains unclear which neuronal subpopulations within the CeA and which CeA efferents influence ethanol consumption (Gilpin *et al*, 2015). One CeA neuron subpopulation that may regulate ethanol phenotypes are the neurons that produce the 13 amino-acid neuropeptide neurotensin (NTS). Indeed, considerable evidence suggests that NTS systems are

critical for reward and anxiety processes (Cáceda *et al*, 2006; Leinninger *et al*, 2011; Fitzpatrick *et al*, 2012; Prus *et al*, 2014, 2014; McHenry *et al*, 2017), and global manipulations of the NTS system disrupt ethanol-related phenotypes (Lee *et al*, 2010, 2011). The majority of studies investigating NTS-expressing neurons, however, focus on those that project from the lateral hypothalamus (LH) to the ventral tegmental area (VTA) and on NTS interactions with dopamine (Binder *et al*, 2001; Kempadoo *et al*, 2013; Leinninger *et al*, 2011; McHenry *et al*, 2017).

Little is known about the role that CeA projections to the hindbrain play in the context of ethanol consumption. Early studies found that the CeA projection to the hindbrain's parabrachial nucleus (PBN) contains NTS+ fibers (Moga and Gray, 1985). The PBN plays a role in the development of conditioned taste aversion (Carter *et al*, 2015; Grigson *et al*, 1998), as well as in fluid satiation (Ryan *et al*, 2017). Additionally, the PBN has been shown to be activated by intraperitoneal injections of ethanol (Chang *et al*, 1995; Thiele *et al*, 1996). The PBN, in turn, sends projections back to the CeA that suppress food consumption (Carter *et al*, 2013). In order to investigate the complex relationship between the CeA and PBN and better understand the role of the CeA-NTS neuronal subpopulation in ethanol consumption and appetitive behaviors, we utilized NTS-*ires*-cre mice (Leinninger *et al*, 2011) in conjunction with region-directed genetic lesioning, optogenetic stimulation, and behavioral assays.

Methods

Subjects, stereotaxic surgery, virus injection and fiber implantation *Mice* All procedures were conducted in accordance with the Guide for the Care and Use of Laboratory Animals, as adopted by the NIH, and with approval of an Institutional Animal Care and Use Committee at UNC-Chapel Hill. Adult male (>22g) NTS-*ires*-cre mice (Leinninger *et al*, 2011) (Jackson Laboratories, Bar Harbor, ME) were used for all experiments. Animals were maintained on a reverse 12 hour light cycle with *ad libitum* access to food and water (unless noted). *Surgery* Mice were anesthetized with inhaled isoflurane (1-3%) and placed in a stereotaxic frame (David Kopf, Germany). For all experiments coordinates for the CeA were as follows (from Bregma, in mm): ML: $\pm$ 2.95, AP: - 1.1, DV: - 4.8, for the PBN: ML $\pm$ 1.4, AP: -5.4, DV: -4.0 (optical fibers). 300 nL of AAV5-

Ef1α-FLEX-taCasp3-TEVp (denoted as: CeA^{NTS}::casp) , AAV5-Ef1α-ChR2-eYFP (denoted as: *NTS*::ChR2 or *NTS*$^{CeA\rightarrow PBN}$::ChR2) , or AAV5-Ef1α-eYFP (denoted as: *NTS*::eYFP or *NTS*$^{CeA\rightarrow PBN}$::eYFP) was infused into the CeA at a rate of 100 nL/min. Optical fibers were constructed as previously described (Sparta *et al*, 2011). Mice were allowed to recover for at least 4 weeks prior to experimentation (8 weeks for optogenetic experiments) to ensure adequate expression of virally encoded genes, and lesioning of target neurons or protein incorporation into the membrane. All viruses were made by the UNC Viral Vector Core (Chapel Hill, NC) or the Stanford Viral Vector (Palo Alto, NC). Following behavioral studies, animals with ChR2-eYFP construct were perfused, and brains were sliced to verify expression of virus. Animals with no viral expression in either CeA were removed (n=1), while animals with either bilateral or unilateral viral expression were included in the analysis as our pilot data indicated that unilateral expression of the virus was sufficient to drive real-time place preference (RTPP) behavior (data not shown). Animals expressing the Caspase construct were euthanized and brains were flash frozen for validation using fluorescent in situ hybridization (FISH, see below) and compared to their eYFP controls.

Fluorescent *in situ* hybridization Mice were anesthetized (isoflurane), decapitated, and brains were flash frozen on dry ice. 12 µm slices were made using a Leica cryostat (CM 3050S, Germany). FISH was performed using probes constructed against PKCδ, CRF, CRFR1 (type-6, fast blue) and NTS (type 1, fast red) and reagents in the View RNA kit (Affymetrix, Santa Clara, CA). Slides were counterstained with DAPI.

Immunohistochemistry As previously described (Pleil *et al*, 2015), mice were perfused with 4% paraformaldehyde (in 0.01 M PBS), brains were removed and allowed to fix for 24 hours followed by cryoprotection in 30% sucrose/PBS. Subsequently brains were sliced at 40 µm on either the CM 3050S or the VT1000 (Leica, Germany). Sections were incubated overnight at 4°C in blocking solution containing primary antibody – anti-sheep tyrosine hydroxylase 1:500 (Pel Freeze), rabbit anti-neurotensin 1:500 (ab43833, Abcam). The following day, sections were incubated in fluorescence-conjugated donkey anti-rabbit IgG Alexa Fluor 647 secondary antibody (1:800, Jackson Immuno) for 2 hr in darkness. 405 neurotrace or DAPI was used as a counterstain.

Microscopy Images were collected and processed on a Zeiss 710, 780 or 800 a using 20X/0.8 objective and the Zen software (Carl Zeiss, Germany). Image J/Fiji was used for cell counting and data analysis.

Slice preparation and whole-cell electrophysiology As previously described (Pleil *et al*, 2015), animals were anesthetized (isoflurane or euthosol) and decapitated. Brains were removed and sliced at a thickness of 200 µm (hindbrain) or 300 µm (CeA) using a Leica VT1200 or VT1000 (Germany) in ice-cold high-sucrose low Na+ artificial cerebral spinal fluid (ACSF in mM: 194 sucrose, 20 NaCl, 4.4 KCl, 2 $CaCl_2$, 1 $MgCl_2$, 1.2 NaH_2PO_4, 10 glucose, 26 $NaHCO_3$) that had been oxygenated (95% O2, 5% CO2) for a minimum of 15 min. Following slicing, brains were allowed to equilibrate in normal ACSF (in mM: 124 NaCl, 4.4 KCl, 2 $CaCl_2$, 1.2 $MgSO_4$, 1 NaH_2PO_4, 10 glucose, 26 $NaHCO_3$, 34º C) for at least 30 minutes. Next, slices were transferred to the electrophysiology rig and allowed to equilibrate in oxygenated ACSF (28-30 ºC) perfused at 2 mL/min for an additional 30 minutes. Recordings examining cell excitability were performed in current clamp using K-gluconate intracellular recording solution (K-gluconate 135, NaCl 5, $MgCl_2$ 2, HEPES 10, EGTA 0.6, Na_2ATP 4, Na_2GTP 0.4). Recordings examining synaptic currents were made either in CsCl intracellular solution (130 CsCl, 1 EGTA, 10 HEPES, 2 ATP, 0.2 GTP) or CsMethanosulfonate (in mM: 117 Cs methanesulfonic acid, 20 HEPES, 0.4 EGTA, 2.8 NaCl, 5 TEA, 2 ATP, 0.2 GTP). CsCl recordings were conducted in kynurinic acid (3mM) to block glutamatergic currents.

Blood Ethanol Content Blood ethanol content (BEC) was measured by administering a dose of 2.0 g/kg (20% ethanol w/v, *i.p.*). Mice were restrained (<2 min) in plexiglass tubes (Braintree Scientific, Braintree, MA) and a scalpel was used to make a small nick in the mouse tail. Blood was collected in a heparinized capillary tube at 30 and 60 minutes following the injection and transferred to a heparinized collection tube, which was then spun down. The plasma was then analyzed for BEC using an Analox-G-5 analyzer (Analox Instruments, Lunenbug, MA)

Ethanol Drinking Paradigms *2-bottle choice* In their homecage, mice were given 24 hour access to a bottle of ethanol (3%, 6%, 10% ethanol, unsweetened) and a bottle of water at 3 days/dose. Measurements of ethanol consumption and water consumption were taken every 24 hours. *Intermittent Access (IA)* was performed as described by Hwa *et al* (Hwa *et al*, 2011). Briefly, mice were allowed access to both a bottle of 20% (w/v) ethanol (unsweetened) and water in their homecage on Monday, Wednesday, and Friday. On other days, they only had access to 2 bottles of water. Bottles were rotated daily to ensure that animals did not associate ethanol or water with a particular side of the cage.

Locomotor and Anxiety Assays All locomotor and anxiety assays were performed using the Ethovision XT tracking software (Noldus Information Technology, Netherlands) to measure location, distance moved, and velocity.

RTPP Mice were placed in an apparatus (50 x 50 x 25 cm) that was divided down the middle with a door for exploration on both sides, and no distinguishing features on either side. For 20 minutes, mice were allowed to explore the apparatus and received optical stimulation (20 Hz, 473 nm, 10 mW, Aurdino UNO, or Master 8, AMP Instruments, Israel) on one side (counterbalanced) and no stimulation on the other side.

oICSS Mice were food-restricted to 80% of their normal food intake for 2 days before optical intracranial self-stimulation (oICSS). They were tethered to the laser and placed in the chamber (15.9 cm x 14.0 cm x 12.7 cm; MedAssociates, VT, USA) for 1 hour. Both nose ports (active and inactive) were baited with a very small amount portion of their normal feed to encourage exploration. A dim house light flashed when the animal had poked the active port along with 5 seconds of stimulation during which time further pokes had no effect (40 Hz, 473 nm, 10 mW).

Open field. Mice were allowed to explore the open field (50 x 50 cm) for 30 minutes where distance traveled, and velocity were measured (Ethovision, Noldus, Amsterdam).

Light-dark box. Mice were placed into the dark enclosed side of the apparatus (Med Associates) and time spent in the light side and entries to the light were monitored for 15 minutes (Ethovision, Noldus, Amsterdam).

Elevated Plus Maze. Mice were placed in the center of the apparatus at the beginning of the test. CeA^{NTS}::casp and control mice were given 5 minutes to explore the open arm, closed arm, and center portion of the maze, and time spent in arms versus center and number of entries were monitored. *NTS*$^{CeA\rightarrow PBN}$::ChR2 and control mice were similarly monitored but given 5 minutes to explore the maze without stimulation, 5 minutes with stimulation (20 Hz, 473 nm, 10 mW) and an additional 5 minutes without stimulation (Ethovision, Noldus, Amsterdam).

Marble burying. 12 marbles were placed on a 5 cm deep layer of corn cob bedding in a standard size mouse cage (39x20x16 cm) in a grid-like fashion. Mice were then placed in the cage for 30 minutes and the degree of marble burying was hand-scored. If a marble was more than ½ way buried it was considered buried. The experimenter was blinded to the mouse treatment prior to the experiment.

Novelty-suppressed feeding. Mice were singly-housed a week prior to testing. 48 hours prior to testing, animals were allowed to consume a fruit-loop in their homecage. Food was then removed from the homecage for 24 hours. Mice were then placed in a corner of an open field (26.7x48.3 cm) at the center of which was a fruit loop on filter paper. Latency to feed was measured as the time required for the mouse to begin to consume the fruit loop. If the mouse had not approached the fruit loop after 10 min, it was removed from the open field and scored as 10 min. Immediately following, the mouse was returned to its homecage and allowed to freely consume fruit loops for 10 min. If the mouse did not consume any fruit loops in the cage, it was not included for this measurement.

Statistical Analysis

Data are presented as mean ± SEM. Significance is presented as *p<0.05, **p<0.01, ***p<0.001, ****p<0.0001. All statistical analyses were performed using GraphPad Prism version 6.02 for Windows, GraphPad Software, La Jolla California USA, www.graphpad.com.

Data was first tested for normality using the D'Agostino-Pearson test. Where data was not normal, a Wilcoxon matched-pairs test was performed. If data was normal, a Student's t-test, paired t-test or matched 2-way ANOVA was performed where appropriate. If a significant interaction was detected in the 2-way ANOVA, a post hoc Bonferroni test was performed.

One *NTS*^{CeA}::eYFP (control) animal was removed from the caspase drinking studies due to extremely low alcohol consumption, never reaching higher than a 2.1 g/kg average per week, and its preference for alcohol was greater than 2 standard deviations from the mean for control animals. One *NTS*$^{CeA->PBN}$::ChR2 was removed from the water-drinking phenotyper experiment. Stimulation-day drinking for this mouse was a ROUT outlier from all other drinking days (stim and non-stim, *NTS*$^{CeA->PBN}$::ChR2 and *NTS*$^{CeA->PBN}$::eYFP).

Results

Neurotensin neurons in the central amygdala express a variety of markers

We first explored how *Nts*-expressing neurons overlap with other previously described genetically-defined populations in the central amygdala (CeA). Using dual fluorescent *in situ* hybridization (FISH) across the entire CeA (approx. bregma -0.8 to -1.9 mm), we found that CeA-NTS neurons are almost exclusively a subpopulation of protein kinase c delta (PKCδ) and corticotropin-releasing factor (CRF) expressing neurons (Supplementary Figure 1A-B), two populations that have been reported to have limited overlap (Cai *et al*, 2014). CeA-NTS neurons also express CRF-receptor 1 mRNA (*Crfr1*; Supplementary Figure 1C). Additionally, approximately two-thirds of CeA-NTS labeled neurons also express preprodynorphin mRNA (*Ppdyn*; Supplementary Figure 1D), the precursor of the endogenous ligand of the kappa opioid receptor (Chavkin *et al*, 1982). As CRF and dynorphin systems in the CeA both play a role in ethanol consumption (Lowery-Gionta *et al*, 2012; Anderson and Becker, 2017), these data suggested that manipulating the CeA-NTS subpopulation may also influence ethanol-related behaviors.

Ablation of neurotensin neurons in the central amygdala decreases ethanol consumption

To determine if CeA-NTS neurons play a role in ethanol-related behavior, we utilized NTS-*ires*-cre-recombinase (NTS-cre) mice (Leinninger *et al*, 2011) in conjunction with viral manipulations in the CeA. First, we validated the fidelity and penetrance of Cre in the CeA of this line. Using FISH (Supplementary Figure 1F), we double-labeled *Nts* and *Cre* mRNA in CeA slices from 5 separate NTS-Cre mice. We found that 61.4% of *Nts* mRNA-expressing cells (241.2 $\pm$ 29.7 *Nts*+ cells per slice) also expressed *Cre* (145.4 $\pm$ 23.7 *Nts*+*Cre*+ cells per slice,) and we found that 82.2% of *Cre* mRNA-expressing cells (173.2 $\pm$ 22.8 *Cre*+ cells per slice) also expressed *Nts* mRNA.

Next, we injected a cre-dependent virus encoding a modified Caspase 3 and TEV protease (AAV5-Ef1a-Flex-taCasp-TEVp; (Morgan *et al*, 2014; Yang *et al*, 2013)) into the CeA of NTS-*ires*-cre mice to selectively lesion CeA-NTS neurons (NTS^{CeA}::casp, Figure 1A). This strategy resulted in a 51.7% reduction in NTS-positive cells in the CeA (measured by FISH; wild-type: 171.9 $\pm$ 3.4 cells, caspase: 83.0 $\pm$ 10.0 cells) and a 40.9% reduction in CeA-NTS immunoreactivity (ir; wild-type: 43.3 $\pm$ 3.2 a.u., caspase: 25.6 $\pm$ 1.3 a.u.), without altering NTS-ir in the neighboring lateral hypothalamus (Figure 1B-E). This lesion of CeA-NTS neurons did not alter locomotor

behavior, anxiety-like behavior, body weight, or ethanol metabolism, when compared to controls that were injected with cre-dependent eYFP (*NTS*^{CeA}::eYFP, Supplementary Figures 2-3).

Due to the importance of the CeA in ethanol consumption and reward (Gilpin *et al*, 2015), we next investigated if the loss of CeA-NTS neurons would alter voluntary ethanol consumption in a continuous 2-bottle choice paradigm. *NTS*^{CeA}::casp mice showed significant decreases in ethanol consumed in 24-hour 2-bottle choice drinking when compared to *NTS*^{CeA}::eYFP (Figure 1F; Two-way ANOVA: interaction, $F_{(2,42)}$= 6.340, p=0.0039; ethanol concentration, $F_{(2,42)}$=98.23, p<0.0001; ablation, $F_{(1,21)}$=16.52, p=0.0006), with no effect of preference for the ethanol bottle (Figure 1G; Two-way ANOVA: interaction, $F_{(2,42)}$=1.793, p=0.1790; ethanol concentration, $F_{(2,42)}$=7.727, p=0.0014; ablation, $F_{(1,21)}$=3.283, p=0.0843). *NTS*^{CeA}::casp animals also showed decreased liquid consumption at lower ethanol concentrations, which was driven by increased total drinking by the *NTS*^{CeA}::casp mice at lower ethanol concentrations (Figure 1H; Two-way ANOVA: interaction, $F_{(2,42)}$=6.551, p=0.0033; ethanol concentration, $F_{(2,42)}$=47.02, p<0.0001; ablation, $F_{(1,21)}$=9.208, p=0.0063). To determine whether *NTS*^{CeA}::casp mice showed differences in liquid consumption compared to controls, we measured water drinking over 5 days. *NTS*^{CeA}::casp mice drank the same levels of liquid as *NTS*^{CeA}::eYFP mice (Figure 1I; Two-way ANOVA: interaction, $F_{(4,44)}$=2.459, p=0.0593; day, $F_{(4,44)}$=2.714 , p=0.0418; ablation, $F_{(1,11)}$=1.005, p=0.3377), confirming that this manipulation affects ethanol consumption as opposed to general liquid consumption.

We next examined whether ablation of *NTS*^{CeA} neurons would still impact alcohol consumption, and perhaps preference, in a drinking paradigm with higher levels of intake. We used an intermittent access (IA) drinking paradigm in an attempt to engender higher levels of drinking. In this paradigm, animals have access to both a 20% ethanol bottle and a water bottle on Monday, Wednesday, and Friday, with water only on other days over the course of 7 weeks. *NTS*^{CeA}::casp mice again showed significant decreases in ethanol consumed across all weeks as compared to *NTS*^{CeA}::eYFP (Figure 2A; Two-way ANOVA: interaction, $F_{(6,126)}$=0.4321, p=0.8564; week, $F_{(6,126)}$=2.539, p=0.0235; ablation, $F_{(1,21)}$=11.19, p=0.0031) as well as cumulative ethanol consumption (Figure 2B; Two-way ANOVA: interaction, $F_{(20,380)}$=13.53, p<0.0001; day, $F_{(20,380)}$= 194.5, p<0.0001; ablation, $F_{(1,19)}$= 11.69, p=0.0029. Bonferroni-corrected post-hoc test shows significant difference between *NTS*^{CeA}::casp and *NTS*^{CeA}::eYFP at days 26 through 47). At the same time, total liquid consumed was

unaffected whether measured by week (Figure 2C; Two-way ANOVA: interaction, $F_{(6,126)}$=1.525, p=0.1752; week, $F_{(6,126)}$=8.358, p<0.0001; ablation, $F_{(1,21)}$=0.00005215, p=0.9943) or cumulatively (Figure 2D; Two-way ANOVA: interaction, $F_{(20,420)}$=0.1298, p>0.9999; day, $F_{(20,420)}$=861.7, p<0.0001; ablation, $F_{(1,21)}$=0.01703, p=0.8976). *NTS*^{CeA}::casp mice also showed significantly decreased preference for the ethanol bottle (Figure 2E; Two-way ANOVA: interaction, $F_{(6,126)}$=0.7778, p=0.588; week, $F_{(6,126)}$=3.992, p=0.0011; ablation, $F_{(1,21)}$=15.88, p=0.0007). Lastly, we compared total amount consumed at the end of the 7 weeks of IA. *NTS*^{CeA}::casp mice consumed significantly less total ethanol than *NTS*^{CeA}::eYFP mice (Figure 2F; Unpaired t-test t(21)=3.413, p=0.0026), with no detectable difference in total liquid consumed (Figure 2G; Unpaired t-test: t(21)=0.04085, p=0.9678). These experiments suggest that CeA-NTS neurons have a role in models of both lower and higher levels of alcohol consumption.

CeA-NTS neurons send a dense projection to the parabrachial nucleus (PBN)

To begin to examine the targets of CeA-NTS neurons, we injected a cre-dependent virus expressing channelrhodopsin-2 tagged with eYFP (ChR2-eYFP) into the CeA of NTS-*ires*-cre mice (Figure 3A-B). Using whole-cell *ex vivo* slice electrophysiology, we found that 473 nm light stimulation (20 Hz, 5 ms pulse, LED, Thor Labs) evoked action potentials in these cells (Supplementary figure 4A). We observed a robust projection from CeA-NTS neurons to the hindbrain near the 4th ventricle with fluorescence expression restricted to the PBN and the lateral edge of the locus coeruleus (LC, Figure 3C). We found significantly greater fluorescence expression in the PBN versus the LC (Figure 3D; Unpaired t-test: t(6)=14.59, p<0.0001), but since LC neurons extend long dendritic processes (Swanson, 1976), we next determined where CeA-NTS neurons make functional synaptic connections within the hindbrain. Monosynaptic input was isolated in whole-cell patch clamp recordings with TTX (500 µM) and 4-AP (100 mM). 473 nm light stimulation of CeA-NTS terminals induced an optically-evoked inhibitory post-synaptic current (IPSC) in both the medial and lateral PBN which was blocked by the GABAA receptor antagonist gabazine (10uM), while no inhibitory or excitatory synaptic currents were observed in the LC (Figure 3E-F, Supplementary figure 4B), similar to what was observed with the CeA-CRF projections (McCall *et al*, 2015). These data suggest that the CeA-NTS neurons make functional inhibitory synaptic connections in the PBN (11 of 13 cells) but not the LC (0 of 10, n=6 mice). We also observed a weaker fluorescent projection to the dorsal and ventral bed nucleus of the stria terminalis (BNST)

where 5 of 9 cells (2 dorsal, 3 ventral) exhibited an optically evoked IPSC (Supplementary figure 5A-B), as well as local connections in the CeA (Supplementary figure 4C representative trace). In order to determine whether CeA-NTS projections to the BNST and PBN originated at the same cell bodies, we injected the retrograde tracer Alexa-488 CTXb into the PBN, and Alexa-555 CTXb into the BNST of the same animal. We found minimal overlap between BNST- and PBN- projecting neurons (1.6%, Supplementary figure 5C-D) suggesting that these are distinct cell populations.

CeA-NTS projection to the parabrachial nucleus (PBN) is reinforcing

The PBN is engaged by ethanol (Thiele *et al*, 1996), regulates consummatory behavior (Douglass *et al*, 2017), and sends reciprocal connections to the CeA (Carter *et al*, 2013). Because of the robust projection from the CeA-NTS neurons to the PBN, we wanted to directly examine how stimulation of this pathway impacts behavior. Additionally, the manipulations of CeA-NTS neurons described above suggested that they may influence motivated behaviors. To investigate the impact of activation of this projection on behavior, we expressed cre-dependent ChR2-eYFP in CeA-NTS neurons and implanted fibers just dorsal to the PBN (*NTS*$^{CeA\rightarrow PBN}$::ChR2-eYFP, Figure 3A, 3G).

To probe if stimulation of the *NTS*$^{CeA\rightarrow PBN}$ pathway altered affective valence, we examined response to photostimulation in the real-time place preference (RTPP) assay (Jennings *et al*, 2013b). Photo-stimulation of these fibers at 20 Hz induced a significant RTPP in *NTS*$^{CeA\rightarrow PBN}$::ChR2-eYFP mice, but not in *NTS*$^{CeA\rightarrow PBN}$::eYFP controls, suggesting that these neurons convey positive valence (Figure 3H-I; Unpaired t-test: $t(25)=6.128$, $p<0.0001$). Optical stimulation significantly increased the distance traveled on the stimulation-associated side of the apparatus (Supplementary figure 6A; Wilcoxon matched-pairs signed rank test: control W= -28, p= 0.2402; ChR2 W= -105, p=0.0001), without altering velocity (Supplementary figure 6B; Wilcoxon matched-pairs signed rank test: control W= -34, p= 0.1475; ChR2 W= 85, p=0.0052). *NTS*$^{CeA\rightarrow PBN}$::ChR2 mice also performed optical intracranial self-stimulation (oICSS) for 40 Hz stimulation of this projection (Figure 3J; Wilcoxon matched-pairs signed rank test: control W= -20, p= 0.3379; ChR2 W= -89, p= 0.0005). Similar to the lack of effect on anxiety-like behavior noted with *NTS*^{CeA}::casp mice, optical activation of the *NTS*$^{CeA\rightarrow PBN}$::ChR2 pathway did not alter behavior in the elevated plus maze either in open arm entries

(Supplementary figure 6C; Two-way ANOVA: interaction $F_{(2,27)}$=0.01082, p=0.9892; stimulation, $F_{(2,27)}$=0.1085, p=0.8976; virus type, $F_{(1,27)}$= 0.4477, p=0.5091) or in time spent in the open arm (Supplementary figure 6D; Two-way ANOVA: interaction $F_{(2,27)}$= 0.6265, p=0.5421; stimulation, $F_{(2,27)}$= 3.034, p=0.0648; virus type, $F_{(1,27)}$= 0.6867, p=0.4146), indicating that this pathway modulates reward-associated behavior but does not alter anxiety-like phenotypes.

Stimulation of the CeA-NTS projection promotes alcohol consumption

We next examined the impact of photostimulation on ethanol consumption in *NTS*$^{CeA→PBN}$::ChR2 mice. Mice were habituated to Ethovision Phenotyper boxes (Noldus) over the course of 4 days for 3 hours each, with 6% ethanol (in bottle with attached Lick-O-Meter) and food available. We tested 6% ethanol because it was the dose where our mice exhibited the highest preference, and the first dose where there was a significant difference in the *NTS*^{CeA}::casp mice in the 2-bottle choice drinking (Figure 1F-G). Over the following 4 days, mice were placed in the same boxes, again with 6% ethanol and their standard mouse chow, and either received optical stimulation across 3 hours (20 Hz, 5 min on-off cycles, see Figure 4A), or received no stimulation (counterbalanced). Prior to and after each session, mice had *ad libitum* water and chow. *NTS*$^{CeA→PBN}$::ChR2 and *NTS*$^{CeA→PBN}$::eYFP mice showed similar levels of drinking during habituation days (Supplementary figure 7). We found that 473 nm, 20 Hz, 10 mW optical stimulation of the *NTS*$^{CeA→PBN}$ pathway increased consumption of 6% ethanol (Figure 4B; Wilcoxon matched-pairs signed rank test: control W=-20, p=0.4131; ChR2 W=61, p=0.0327) as compared to non-stimulation days, whereas stimulation of *NTS*$^{CeA→PBN}$::eYFP mice did not alter ethanol consumption. On the days that the mice received stimulation, we found that significantly more ethanol consumption (number of licks) occurred during the 5-min laser on versus laser off phases (Figure 4C; Wilcoxon matched-pairs signed rank test: control W= -20, p= 0.4131; ChR2 W= 61, p= 0.0327). Surprisingly, in this experimental paradigm, *NTS*$^{CeA→PBN}$::ChR2 mice decreased chow consumption on days when they received stimulation (Figure 4C; Two-way ANOVA: interaction $F_{(1,22)}$=4.313, p=0.0497; virus type, $F_{(1,22)}$=0.5391, p=0.4705; stimulation, $F_{(1,22)}$= 7.387, p=0.0126). In summary, these data show that stimulation of the *NTS*$^{CeA→PBN}$ projection can promote ethanol consumption in freely-moving mice.

We next sought to determine whether this increase in ethanol consumption and concurrent decrease in chow consumption was due to a generalized increase in liquid consumption, a generalized decrease in chow consumption, or an ethanol-specific phenotype. In mice given *ad libitum* food and water, we performed the same experimental paradigm as above (Figure 4A), but with water instead of ethanol. Stimulation of *NTS*$^{CeA→PBN}$::ChR2 mice did not significantly alter water consumption (Figure 5A; Two-way ANOVA: interaction $F_{(1,14)}$=0.9252, p=0.3524; virus type, $F_{(1,14)}$=9.541e-005, p=0.9923; stimulation, $F_{(1,14)}$=1.203, p=0.2913), licks to the bottle (Figure 5B; Wilcoxon matched-pairs signed rank test: control W=13, p=0.2188; ChR2 W=26, p 0.0781), or chow consumption (Figure 5C; Two-way ANOVA: interaction $F_{(1,14)}$=0.5311, p=0.4782; virus type, $F_{(1,14)}$=4.257, p=0.0581; stimulation, $F_{(1,14)}$=1.218, p=0.2883. Together, these data demonstrate an alcohol-specific role for the *NTS*$^{CeA→PBN}$ projection in consumptive behaviors, disassociated from the CeA and PBN's reported roles in general food and liquid consumption.

Discussion

The central nucleus of the amygdala (CeA) is well known to regulate several behaviors associated with alcohol use disorders. The particular genetically defined cell types and circuits that mediate these behaviors, however, are currently unknown. Here we have shown that NTS-expressing neurons in the CeA contribute to voluntary alcohol-consumption in mice. Additionally, our data demonstrate that a subset of these neurons project to the PBN, and that stimulation of this projection is positively reinforcing and leads to increased alcohol consumption. Surprisingly, this stimulation decreases food consumption, but only under conditions where the animal has the option to drink alcohol. Taken together, these data suggest a role for CeA NTS-containing neurons in the positively-reinforcing aspects of alcohol consumption at the expense of food consumption.

CeA neurotensin neurons do not engage anxiety-like behaviors

Our data confirm other reports that CeA-NTS neurons are a subpopulation of neurons that also express CRF, but differ in that we also saw that NTS neurons are a subpopulation of PKCδ mRNA-containing neurons (Kim *et al*, 2017). It is noteworthy that others have observed a small portion of CeA neurons that contain both CRF and PKCδ, which may comprise the NTS expressing cells (Haubensak *et al*, 2010; Cai *et al*, 2014). Here, we also report substantial overlap with cells containing mRNA for ppDyn. Intriguingly, neither ablation of these

neurons nor their excitation altered any tests of anxiety-like behavior (Supplementary figures 3, 6) similar to what has been observed with cell body activation of PKCδ-containing neurons (Cai *et al*, 2014). Data examining the CRF projection to the LC (which is located just medial of the PBN), however, demonstrated that stimulation of this projection engaged anxiety-like behavior via CRF stimulation of CRF-receptor1 (CRFR1), which then induced an increase in the firing rate of LC neurons. These discrepancies could be due to multiple factors: 1. The NTS cells are a subpopulation of CRF mRNA-containing neurons, and it is possible that expression of CRF mRNA does not mean that these cells release CRF protein; 2. Only CRF cells that lack the expression of NTS release CRF in proximity to LC neurons/processes that express CRFR1; or 3. That expression of Cre in these driver lines may target distinct neurons projecting to the hindbrain, as we observe a penetrance of 64% of NTS containing neurons. As CeA neurons expressing PKCδ also did not engage anxiety-like behavior and our data suggest that CeA-NTS neurons comprise the overlap between these two populations, it stands to reason that a subpopulation of CeA-CRF containing neurons do not engage anxiety-like behaviors.

CeA neurotensin neurons promote positive valence and reinforcement

In contrast to what was observed with the CRF-cre projection to the LC discussed above, stimulation of the *NTS*$^{CeA→PBN}$ resulted in behaviors associated with reward and positive valence. Other groups have shown that stimulation of the CeA can increase responding for a laser-paired positive reinforcer and even shift preference towards a non-preferred outcome when paired with stimulation (Robinson *et al*, 2014; Warlow *et al*, 2017). These experiments target the entire CeA, however, and animals do not show intracranial self-stimulation behavior. This has led to a hypothesis that the CeA has a role in amplifying motivation for reward-seeking, but does not have a direct role in reward in and of itself. In comparison, recent work demonstrated that mice will perform oICSS of CeA cell bodies in genetically-defined subpopulations of CeA neurons (Kim *et al*, 2017) and that stimulation of different genetically defined CeA→PBN projection can reinforce behavior (Douglass *et al*, 2017). These data are in line with our finding that animals will perform oICSS and demonstrate real-time place preference for stimulation of the *NTS*$^{CeA→PBN}$ projection (Figure 3J). We posit that stimulation of heterogeneous groups in the CeA may obscure the role of specific projections or genetically-defined subtypes, particularly when they may have reciprocal inhibitory connections.

The role of CeA neurotensin neurons in alcohol and food consumption

The CeA is well known to be engaged by alcohol consumption and is implicated in mediating both the negative and positive reinforcing properties of alcohol (Koob *et al*, 1998; Koob, 2015). In keeping with this, an earlier study from Hyytiä and Koob found that pharmacological inhibition of the CeA reduces ethanol consumption (Hyytiä and Koob, 1995) and amygdalar lesions can cause reductions in alcohol consumption (Möller *et al*, 1997). Our data show that selective lesioning of *NTS*^{CeA} neurons can decrease alcohol intake and reduce preference for alcohol without altering other fluid consumption. Concordant with this finding, we found that optogenetic stimulation of the *NTS*$^{CeA \rightarrow PBN}$ projection increased alcohol consumption during stimulation epochs, but again did not alter consumption of water. This data suggests that stimulation of this projection is related to engagement with the salient stimulus, as opposed to inhibiting the previously described PBN fluid satiation neurons, which would lead to increased overall fluid intake (Ryan *et al*, 2017).

Select populations of the CeA are known to alter the consumption of food. Activation of PKCδ populations reduces food intake (Cai *et al*, 2014), and in contrast, activation of serotonin 5-HT2$_A$ receptor-containing populations increase consumption of food (Douglass *et al*, 2017). In order to exclude that changes in alcohol drinking were due to alterations in general consummatory behavior, and to better mimic the drinking experiments performed in the *NTS*^{CeA}::caspase mice, we measured food consumption during the optogenetic alcohol/water experiments. Interestingly, we observed that when alcohol was present, but not when water was present, stimulation of the *NTS*$^{CeA \rightarrow PBN}$ projection decreased the consumption of food. These data suggest that the effect that we are observing on alcohol is not due to the mice seeking a caloric source or increased fluid, but may be selective for alcohol. Indeed, we hypothesized that the presence of alcohol altered the motivational state of the mice and shifted their desire to consume less food.

Cai et al. show that the PKCδ neurons send a projection to the PBN, but they only observed a small IPSC in 1 out of the 6 neurons recorded, while we observed IPSCs in 13 of 15 cells recorded. We hypothesize that this discrepancy may have been due to recording location. The dorsal-most aspect of the PBN does not appear to receive GABAergic input from the CeA-NTS neurons, as indeed we did not observe current in the 2 dorsal

neurons we patched there, nor does it appear that the more ventrolateral aspect of the PBN (where the pro-anorectic calcitonin gene-related peptide-containing neurons reside) receives a projection from the CeA-NTS neurons. We observed current in 13 cells from the median aspect of both the medial and lateral PBN.

CeA neurotensin neurons, a potential role in salience

There is considerable evidence that stimulating non-specific CeA cell bodies contributes to an increase in the incentive salience associated with a reward (Mahler and Berridge, 2009; Robinson *et al*, 2014; Warlow *et al*, 2017). The data presented here suggests a more nuanced role for the *NTS*$^{CeA\rightarrow PBN}$ pathway than simply driving or suppressing general consumptive states. Particularly, we find that the effects of stimulating the *NTS*$^{CeA\rightarrow PBN}$ projection on food consumption are context- and choice-dependent. When mice are presented with the choice of drinking alcohol or eating food, stimulation of the *NTS*$^{CeA\rightarrow PBN}$ projection increases alcohol consumption at the expense of food consumption. When mice are offered water and food, however, stimulation of this pathway fails to increase or decrease consumption of either substance. In addition, we did not observe differences in growth curves of the *NTS*^{CeA}::casp mice, suggesting that ablation of this pathway does not result in enhanced chow consumption. Our results are additionally interesting because many of the pathways that drive decreases in food consumption are inherently aversive (Jennings *et al*, 2013a; Betley *et al*, 2015), but our results suggest the stimulation of the *NTS*$^{CeA\rightarrow PBN}$ projection exhibits a positive valence and is reinforcing.

CeA to PBN pathway as a pathway for alcohol consumption phenotypes

Mounting evidence points to the amygdala as an important substrate for the actions of ethanol, particularly synaptic modulation of GABAergic signaling (Roberto *et al*, 2004; Herman *et al*, 2013). Much of this work, however, has focused on the consumption of alcohol as a means to alleviate an increase in anxiety-like behavior via negative reinforcement (Koob *et al*, 2014; Anderson and Becker, 2017). Interestingly, using the 20% ethanol IA paradigm, a study from the George lab has shown that discrete neuronal ensembles in the CeA are recruited during abstinence from ethanol, and lesioning these neurons transiently reduces ethanol intake in “non-dependent” rats, with alcohol consumption returning to control levels within a week (de Guglielmo *et al*, 2016). In contrast, our data demonstrate that lesioning the CeA-NTS population decreases drinking with no recovery to control levels. Furthermore, we identify a specific CeA output population,

NTS$^{CeA\rightarrow PBN}$, and show that it promotes alcohol consumption and reward, without modulating anxiety-like behavior. In our experiments, we investigated the *NTS*$^{CeA\rightarrow PBN}$ in animals with relatively brief alcohol experience (habituation days). Future studies will characterize the role of alcohol experience/dependence in modulating *NTS*^{CeA} neurons, and their projections to the PBN.

Our data have demonstrated that NTS-expressing neurons in the CeA bi-directionally control ethanol consumption in mice. Lesioning these neurons decreases ethanol drinking and preference, while stimulating their projections to the PBN increases ethanol drinking in non-dependent mice. Interestingly, neither of these manipulations alters anxiety-like behavior, while stimulation of the *NTS*$^{CeA\rightarrow PBN}$ projection promotes positive valence and reinforcement. Surprisingly, stimulation of this pathway reduces food consumption, but this is dependent on the motivational state of the animal. These data suggest that NTS-expressing CeA neurons, and especially their projection to the PBN, play a significant role in modulation of specific consumptive behaviors and may alter incentive salience.

Acknowledgements

The authors thank Drs. Thomas Kash and Elyse Dankoski for on previous versions of the manuscript. This work was supported by: K01 AA023555 (Z.A.M.), P60 AA011605 (C.W.H., G.D.S)

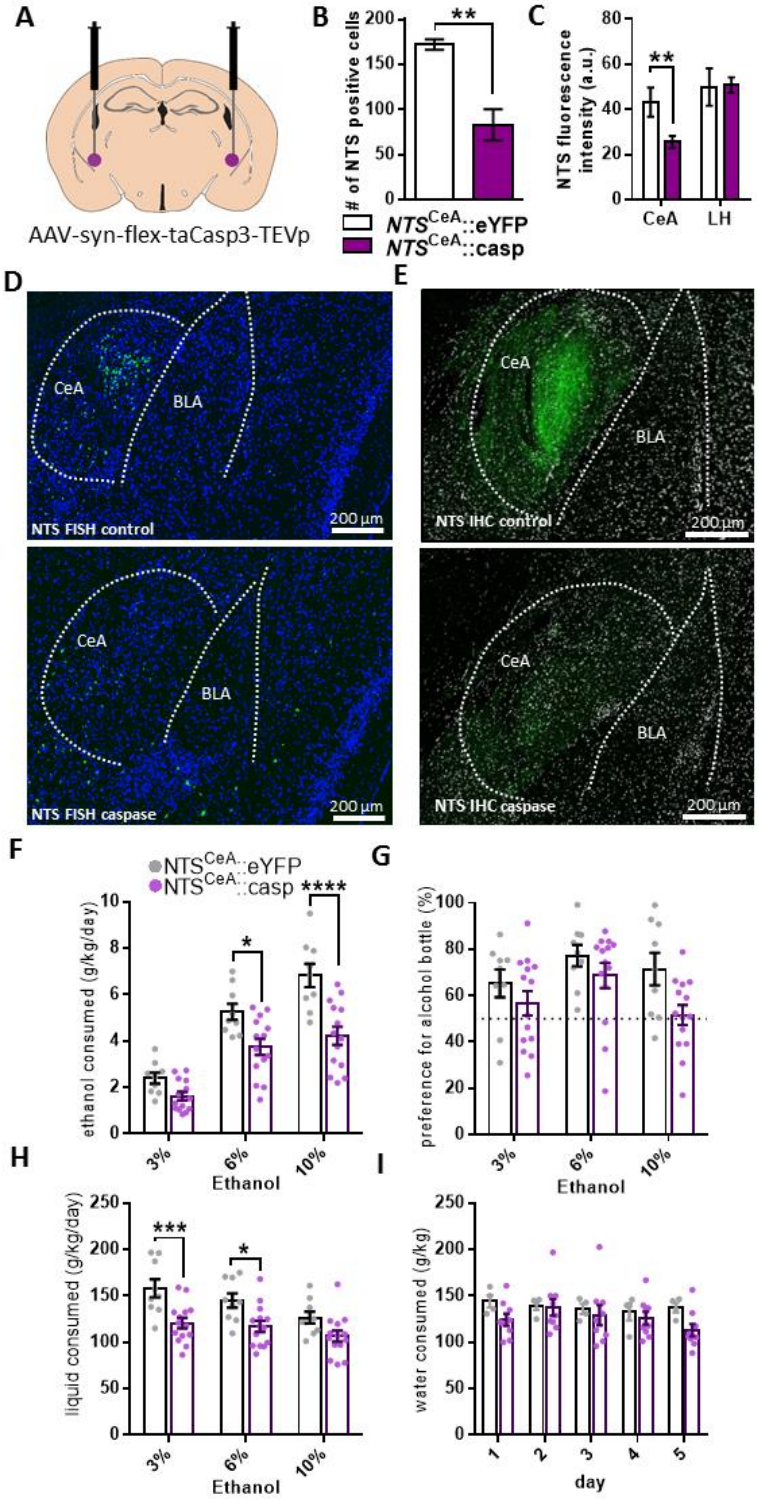

Figure 1 – Ablation of neurotensin neurons in the central amygdala decreases ethanol drinking (a) Diagram of injection site in the CeA AAV-syn-flex-taCasp3-TEVp of NTS-ires-Cre mice.(b) of cells FISH labeled for NTS in the CeA from NTS^{CeA}::casp (purple bars, n=3) and NTS^{CeA}::eYFP animals (white bars, n=3, unpaired t-test: t(4)=8.425, p=0.0011). (c) Quantification of NTS IHC fluorescence intensity in the CeA and LH of NTS^{CeA}::casp (purple bars, n=4) and NTS^{CeA}::eYFP (white bars, n=4). Caspase ablation decreased NTS immunoreactivity in the CeA (unpaired t-test: t(6)=5.090, p=0.0022), but not in the LH (unpaired t-test: t(6)=0.1956, p=0.8514). (d) Representative images of FISH for NTS (green) and DAPI (blue) in NTS^{CeA}::eYFP (upper panel) and NTS^{CeA}::casp (lower panel) mice. (e) Representative images of NTS IHC (green) and DAPI (white) in the CeA of NTS^{CeA}::eYFP (upper panel) and NTS^{CeA}::casp (lower panel) mice. (f) Caspase ablation in the CeA decreases ethanol consumption (NTS^{CeA}::eYFP n = 9, NTS^{CeA}:Casp n= 14; Two-way ANOVA: interaction, $F_{(2,42)}$= 6.340, p=0.0039; ethanol concentration, $F_{(2,42)}$=98.23, p<0.0001; ablation, $F_{(1,21)}$=16.52, p=0.0006). Bonferroni post hoc analysis, *p<0.05, ****p<0.0001). (g) Caspase ablation does not significantly decrease preference for ethanol (ethanol bottle contribution to percent of total liquid consumption). (Two-way ANOVA: interaction, $F_{(2,42)}$=1.793, p=0.1790; ethanol concentration, $F_{(2,42)}$=7.727, p=0.0014; ablation, $F_{(1,21)}$=3.283, p=0.0843). (h) Caspase ablation decreases total liquid consumption compared to controls. (Two-way ANOVA: interaction, $F_{(2,42)}$=6.551, p=0.0033; ethanol concentration, $F_{(2,42)}$=47.02,

p<0.0001; ablation, $F_{(1,21)}$=9.208, p=0.0063). Bonferroni post hoc analysis, *p<0.05, ***p<0.001). (i) 5 days of water drinking shows no effect of caspase ablation. (NTS^{CeA}::eYFP n = 4, NTS^{CeA}:Casp n= 9; Two-way ANOVA: interaction, $F_{(4,44)}$=2.459, p=0.0593; day, $F_{(4,44)}$=2.714, p=0.0418; ablation, $F_{(1,11)}$=1.005, p=0.3377).

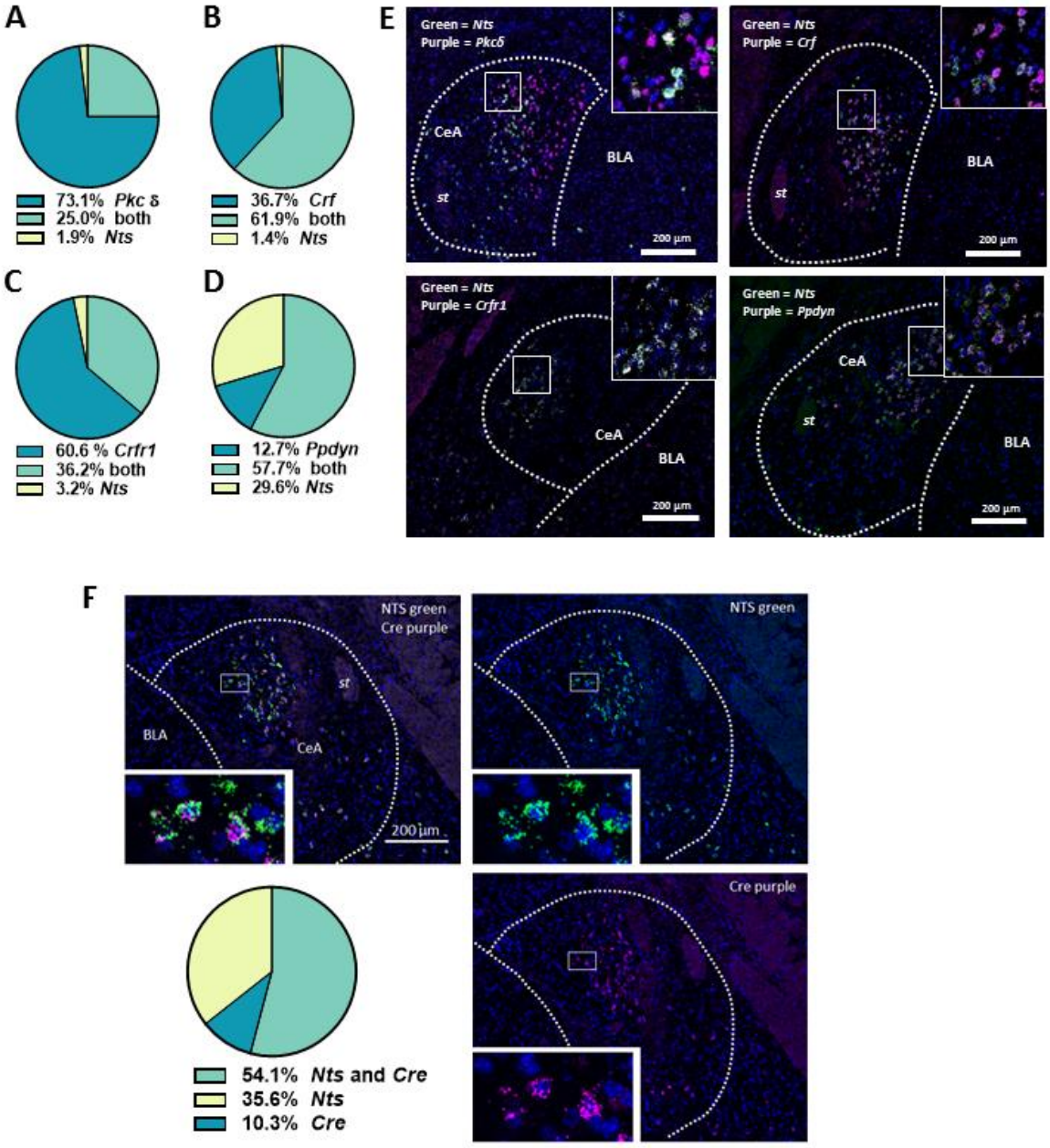

Supplementary Figure 1 – Expression and colocalization of molecular markers (a) Dual FISH of *Nts* (green), *Pkcδ* (purple) and DAPI (blue) in the CeA (st= stria terminalis, BLA = basolateral amygdala, all scale bars 200 µm). The distribution of *Nts* neurons almost completely co-localized with *Pkcδ*, while there were a substantial number of *Pkcδ* neurons that did not express *Nts*. (n = 4 mice, 5-6 slices/mouse) (b) Dual FISH of *Nts* (green), *Crf* (purple), and DAPI (blue) in the CeA. The distribution of *Nts* neurons almost completely co-localized with *Crf*, while there were a substantial number of *Crf* neurons that did not express *Nts*. (n = 3 mice, 5-6 slices/mouse) (c) Dual FISH of *Nts* (green), *Crfr1* (purple), and DAPI (blue) in the CeA. The distribution of *Nts* neurons largely completely co-localized with *Crfr1*. There were a substantial number of *Crfr1* neurons that did not express NTS. (n=4 mice, 5-6 slices/mouse) (d) Dual FISH of *Nts* (green), *Ppdyn* (purple), and DAPI (blue) in the CeA. The distribution of *Ppdyn* neurons largely completely co-localized with *Nts*. There were a substantial number of both *Nts* and *Ppdyn* neurons that did not colocalize. (n=4 mice, 5-6 slices/mouse) (e) Representative images of double-labelled *in situ* for *Nts*/*Pkcδ*, *Nts*/*Crf*, *Nts*/*Crfr1*, and *Nts*/*Ppdyn*. (f) Dual FISH of *Nts* (green), *Cre* (purple), and DAPI (blue) in the CeA. 54.1% of labelled cells were *Nts* and *Cre* positive, 35.6% were *Nts* single-labelled, and 10.3% were *Cre* single-labelled. (n=3 mice, 5-6 slices/mouse)

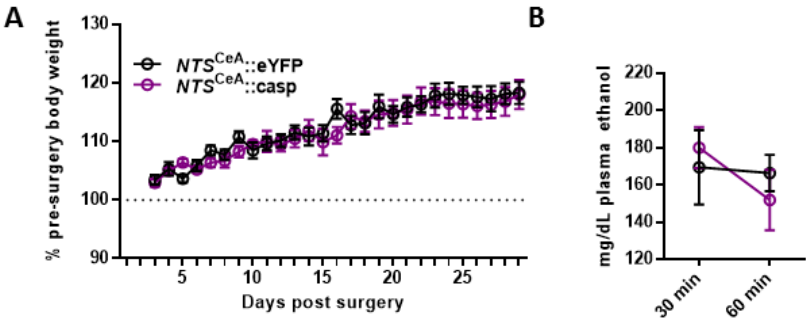

Supplementary figure 2 – Caspase ablation of *NTS*^{CeA} does not alter body weight or blood ethanol content (a) *NTS*^{CeA}::casp mouse weight post-surgery does not differ from *NTS*^{CeA}::eYFP weight (*NTS*^{CeA}::eYFP n = 5, *NTS*^{CeA}:Casp n= 5; Two-way ANOVA: interaction, $F_{(26, 208)}$=0.9646; day, $F_{(26,208)}$= 40.11, p<0.0001, p=0.5180; ablation, $F_{(1,8)}$=0.1154, p=0.7428). (b) Blood alcohol concentrations (BACs) following administration of 2.0 g/kg ethanol in *NTS*^{CeA}::casp (purple circles) and *NTS*^{CeA}::eYFP mice(white circles). The mice did not differ in ethanol metabolism (*NTS*^{CeA}::eYFP n = 5, *NTS*^{CeA}:Casp n= 5; Two-way ANOVA: interaction, $F_{(1,8)}$=1.270, p=0.2924; time, $F_{(1,8)}$=1.964, p=0.1987; ablation, $F_{(8,8)}$=2.538, p=0.1046).

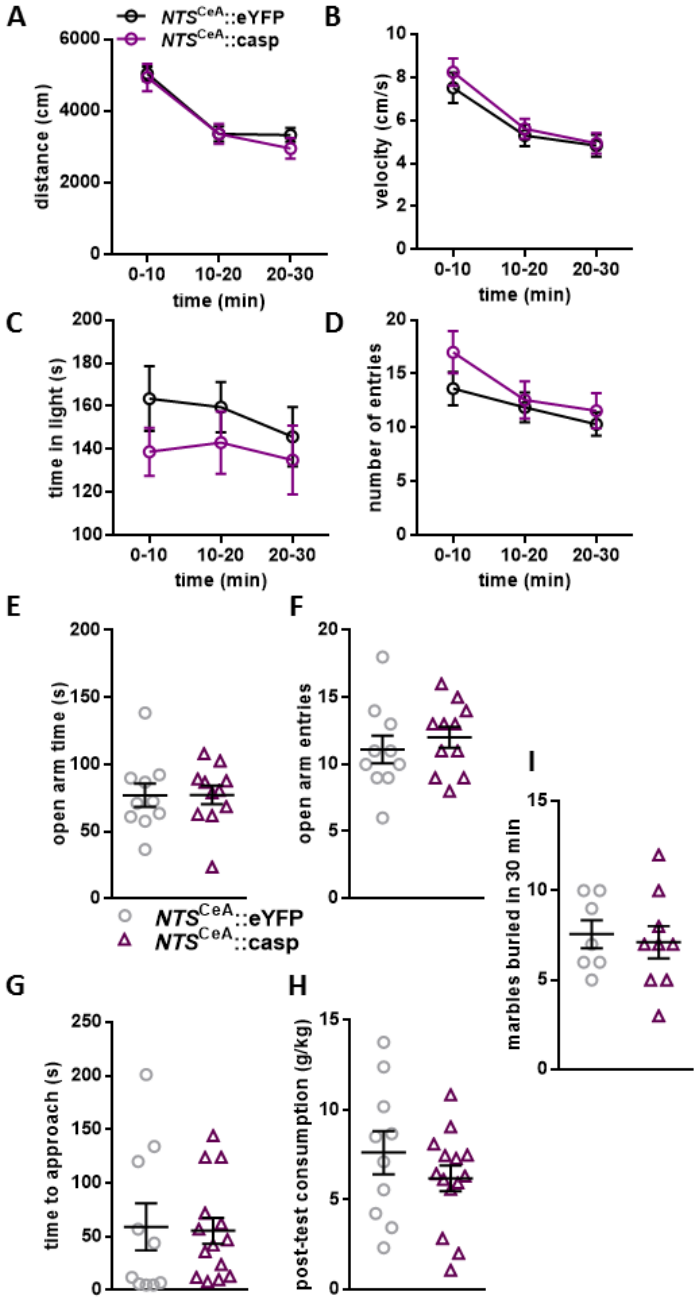

Supplementary Figure 3 – Caspase ablation of *NTS*^{CeA} does not alter anxiety-like behavior (a) Distance traveled in the open field demonstrates no difference between *NTS*^{CeA}::eYFP (n=9, black circles) and *NTS*^{CeA}::casp mice (n=11, purple circles). (Two-way ANOVA: interaction, $F_{(2,36)}$=0.9989 , p=0.3783; time, $F_{(2,36)}$=109.3, p<0.0001; ablation, $F_{(1,18)}$=0.1886, p=0.6693). (b) Velocity in the open field demonstrates no difference between *NTS*^{CeA}::eYFP (n=9, black circles) and *NTS*^{CeA} ::casp mice (n=11, purple circles). (Two-way ANOVA: interaction, $F_{(2,38)}$=0.9970, p=0.3784; time, $F_{(2,38)}$=98.55, p<0.0001; ablation, $F_{(1,19)}$=0.2698, p=0.6095). (c) Time spent in the light side of the light dark box demonstrates no difference between *NTS*^{CeA}::eYFP (n=16, black circles) and *NTS*^{CeA} ::casp mice (n=18, purple circles). (Two-way ANOVA: interaction, $F_{(2,64)}$=0.3707, p=0.6917; time, $F_{(2,64)}$=1.203, p=0.3071; ablation, $F_{(1,32)}$=1.000, p=0.3247). (d) Number of entries into the light side of the light dark box demonstrates no difference between *NTS*^{CeA}::eYFP (n=16, black circles) and *NTS*^{CeA} ::casp mice (n=16, purple circles). (Two-way ANOVA: interaction, $F_{(2,60)}$=1.452, p=0.2422; time, $F_{(2,60)}$=14.63, p<0.0001; ablation, $F_{(1,30)}$=0.7529, p=0.3924). (e) No differences were observed between *NTS*^{CeA}::eYFP (n=10, grey circles) and *NTS*^{CeA}::casp mice (n=11, purple triangles) in time spent in the open arm of the EPM. (Unpaired t-test: t(19)=0.03167, p=0.9751). (f) No differences were observed between *NTS*^{CeA}::eYFP (n=10, grey circles) and *NTS*^{CeA} ::casp mice (n=11, purple triangles) in entries into the open arm of the EPM. (Unpaired t-test: t(19)=0.6992, p=0.4929). (g) No differences were observed between *NTS*^{CeA}::eYFP (n=10, grey circles) and *NTS*^{CeA} ::casp mice (n=14, purple triangles) in time to approach the food in the novelty-suppressed feeding task. (Unpaired t-test: t(22)=0.1597, p=0.8746). (h) No differences were observed between *NTS*^{CeA}::eYFP (n=10, grey circles) and *NTS*^{CeA} ::casp mice (n=14, purple triangles) in food consumed in the 10 minute post-test of the novelty-suppressed feeding task. (Unpaired t-test: t(22)=1.086, p=0.2892). (i) No differences were observed between *NTS*^{CeA}::eYFP (n=7, grey circles) and *NTS*^{CeA} ::casp mice (n=9, purple triangles) in marbles buried during the 30 min marble burying task. (Unpaired t-test: t(14)=0.3716, p=0.7158).

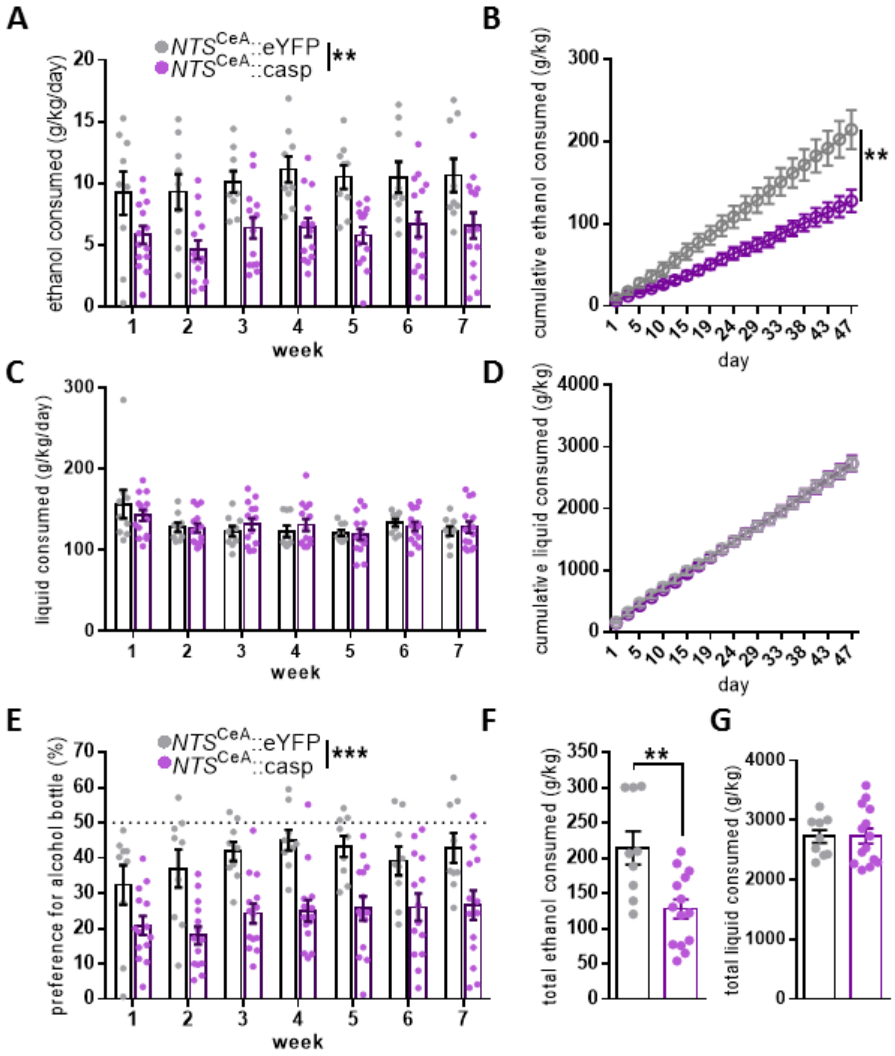

Figure 2– Ablation of neurotensin neurons in the central amygdala decreases ethanol drinking and preference in an intermittent access paradigm (a) NTS^{CeA}::casp mice consume less ethanol than NTS^{CeA}::eYFP mice. (NTS^{CeA}::eYFP n = 9, NTS^{CeA}:Casp n= 14; Two-way ANOVA: interaction, $F_{(6,126)}$=0.4321, p=0.8564; week, $F_{(6,126)}$=2.539, p=0.0235; ablation, $F_{(1,21)}$=11.19, p=0.0031). (b) NTS^{CeA}::casp mice cumulatively consume less ethanol than NTS^{CeA}::eYFP mice across 7 weeks of intermittent access. (Two-way ANOVA: interaction, $F_{(20,420)}$=13.15, p<0.0001; day, $F_{(20,420)}$= 196.2, p<0.0001; ablation, $F_{(1,21)}$= 10.97, p=0.0033). (c) NTS^{CeA}::eYFP and NTS^{CeA}::casp mice consume similar amounts of liquid. (Two-way ANOVA: interaction, $F_{(6,126)}$=1.525, p=0.1752; week, $F_{(6,126)}$=8.358, p<0.0001; ablation, $F_{(1,21)}$=0.00005215, p=0.9943). (d) NTS^{CeA}::eYFP and NTS^{CeA}::casp mice cumulatively consume similar amounts of liquid. (Two-way ANOVA: interaction, $F_{(20,420)}$=0.1298, p>0.9999; day, $F_{(20,420)}$=861.7, p<0.0001; ablation, $F_{(1,21)}$=0.01703, p=0.8976). (e) Caspase ablation decreases preference for the alcohol bottle. (Two-way ANOVA: interaction, $F_{(6,126)}$=0.7778, p=0.588; week, $F_{(6,126)}$=3.992, p=0.0011; ablation, $F_{(1,21)}$=15.88, p=0.0007). (f) Final total ethanol consumption is significantly lower in NTS^{CeA}::casp mice compared to NTS^{CeA}::eYFP mice. (Unpaired t-test t(21)=3.413, p=0.0026). (g) Final total liquid consumption is similar between NTS^{CeA}::eYFP and NTS^{CeA}::casp mice. (Unpaired t-test: t(21)=0.04085, p=0.9678).

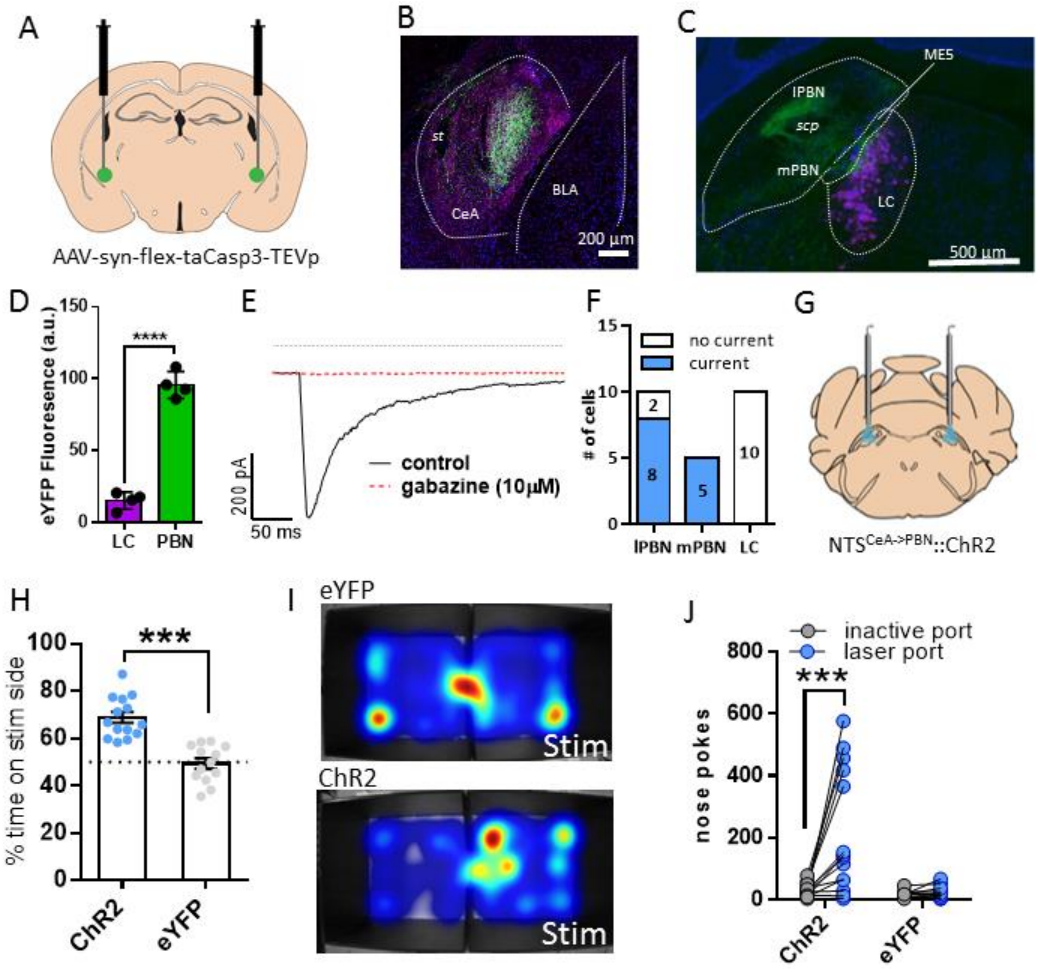

Figure 3– ChR2 Stimulation of the *NTS*$^{CeA\rightarrow PBN}$ projection is reinforcing (a) Diagram of injection site in the CeA of AAV-EF1α-DIO-ChR2-eYFP in the CeA of NTS-ires-cre mice. (b) Representative image of CeA expression of ChR2-eYFP (green) and NTS IHC (purple) in the CeA (st= stria terminalis, BLA = basolateral amygdala, scale bars 200 µm). (c) Representative image of hindbrain, NTS^{CeA}::ChR2-eYFP fibers (green), tyrosine hydroxylase (TH, purple), neurons (blue). (4v= 4th ventricle, ME5 = midbrain trigeminal nucleus, scp = superior cerebellar peduncle) (d) PBN has significantly greater eYFP fluorescence intensity as compared to the LC in NTS$^{CeA\rightarrow PBN}$::ChR2 (n = 4; Unpaired t-test: t(6)=14.59, p<0.0001). (e) Representative trace of oeIPSC in the PBN and its inhibition by gabazine (10 µM) (f) Quantification of cells with light-evoked responses in the lPBN (n = 10 cells), mPBN (n = 5 cells) and LC (n = 10 cells). (g) Diagram of optical fiber placement above the PBN. (h) Percent of time spent on stimulation (20 Hz) side during RTPP (NTS$^{CeA\rightarrow PBN}$::eYFP n = 13, NTS$^{CeA\rightarrow PBN}$::ChR2-eYFP n = 14) Unpaired t-test: t(25)=6.128, p<0.0001). (i) Representative heatmaps of mice location during RTPP.(j) Mouse poking during optical intracranial celf-stimulation (oICSS) (NTS$^{CeA\rightarrow PBN}$::eYFP n = 11, NTS$^{CeA\rightarrow PBN}$::ChR2-eYFP n = 14 Wilcoxon matched-pairs signed rank test: control W= -20, p= 0.3379; ChR2 W= -89, p= 0.0005).

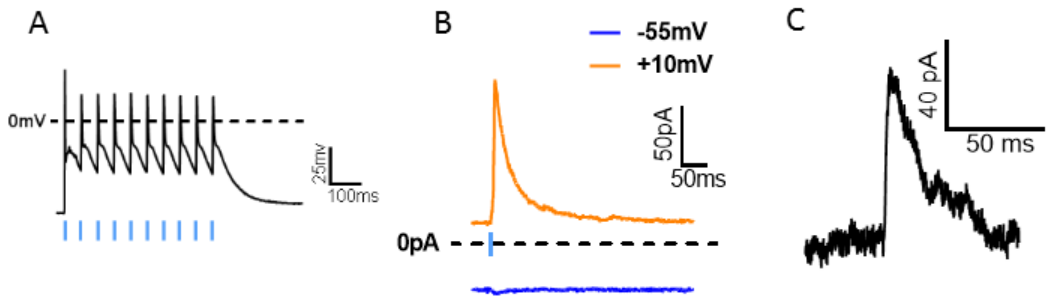

Supplementary figure – 4 Optical stimulation of *NTS*^{CeA}::ChR2-eYFP cell bodies and projections (a) Representative trace of NTS^{CeA}::ChR2 neuron following 20 Hz optical stimulation stimulation. (b) Representative traces of optically evoked synaptic currents in PBN recorded with Cs-Methanosulfonate intracellular. Outward current at +10 mV is indicative of oeIPSC, while lack of current at -55 mV demonstrates the NTS-CeA projection is not glutamatergic. (c) Representative trace of an oeIPSC recorded in the CeA from an eYFP- cell.

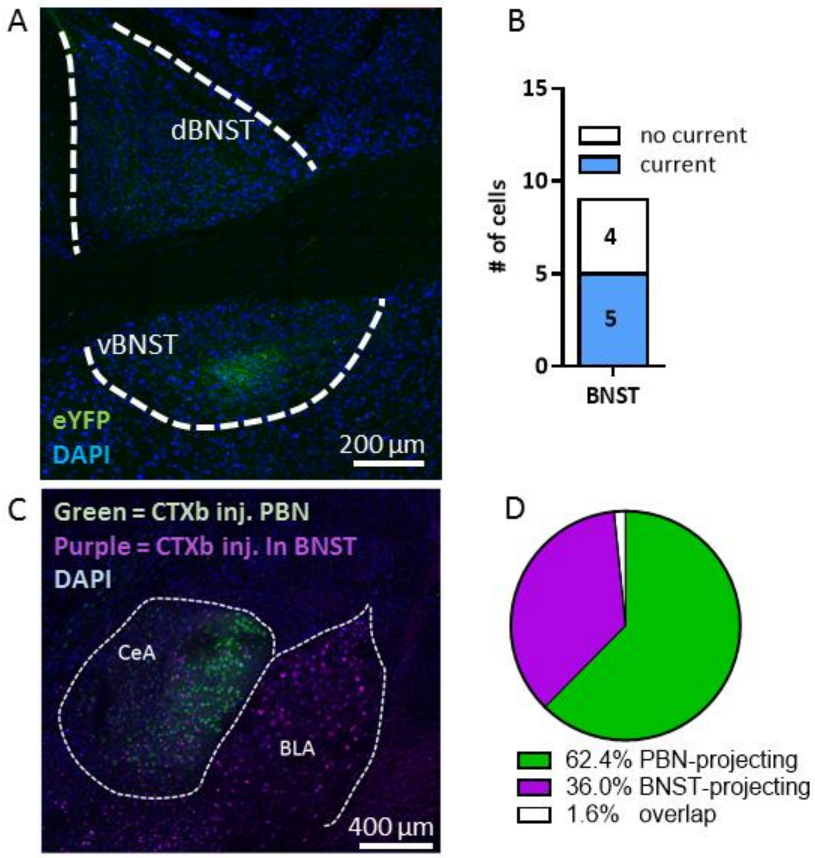

Supplementary figure 5 – Optical stimulation of *NTS*^{CeA}::ChR2-eYFP BNST projections, and PBN/BNST projecting CeA overlap
(a) Representative image of expression of NTS^{CeA}::ChR2-eYFP fibers (green) in the BNST (dBNST = dorsal portion of the bed nucleus of the stria terminalis, vBNST = ventral portion of the bed nucleus of the stria terminalis). (b) Quantification of cells with light-evoked responses in the BNST (n = 9 cells). (c) Representative CeA image of retrograde cholera toxin-b tracing experiment. Green = cells projecting to the parabrachial nucleus (PBN), purple = cells projecting to the BNST. (d) Quantification of cell body fluorescence expression (green and purple ctxb) in the CeA. (n = 3 mice)

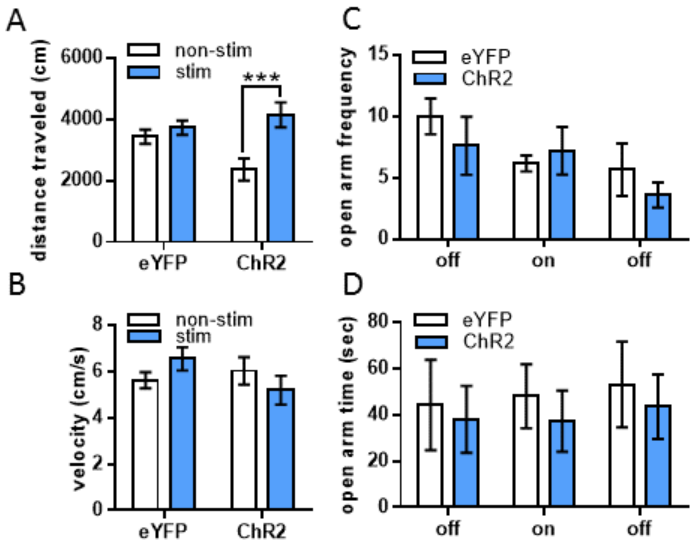

Supplementary figure 6 – *NTS*$^{CeA→PBN}$::ChR2-eYFP stimulation does not engage anxiety-like behavior (a) *NTS*^{CeAàPBN}::ChR2 mice (n=14) traveled significantly greater distance on the stimulation side of the chamber while the *NTS*^{CeAàPBN}::eYFP animals (n=11) did not (Wilcoxon matched-pairs signed rank test: control W=-28, p=0.2402; ChR2 W=-105, p=0.0001). (b) *NTS*^{CeAàPBN}::ChR2 (n=14) and *NTS*^{CeAàPBN}::eYFP mice (n=11) did not have altered velocity during 20 Hz optical stimulation (Wilcoxon matched-pairs signed rank test: control W=-34, p=0.1475; ChR2 W=85, p=0.0052). (c) *NTS*^{CeAàPBN}::ChR2 (n=5) and *NTS*^{CeAàPBN}::eYFP mice (n=6) did not show differences in entries to the open arms of the elevated-plus maze. (Two-way ANOVA: interaction $F_{(2,27)}$=0.01082, p=0.9892, stimulation, $F_{(2,27)}$=0.1085, p=0.8976, virus type, $F_{(1,27)}$=0.4477, p=0.5091). (d) *NTS*^{CeAàPBN}::ChR2 (n=5) and *NTS*^{CeAàPBN}::eYFP mice (n=6) did not show alterations in time spent in the open arms of the EPM. (Two-way ANOVA: interaction $F_{(2,27)}$=0.6265, p=0.5421; stimulation, $F_{(2,27)}$=3.034, p=0.0648; virus type, $F_{(1,27)}$=0.6867, p=0.4146).

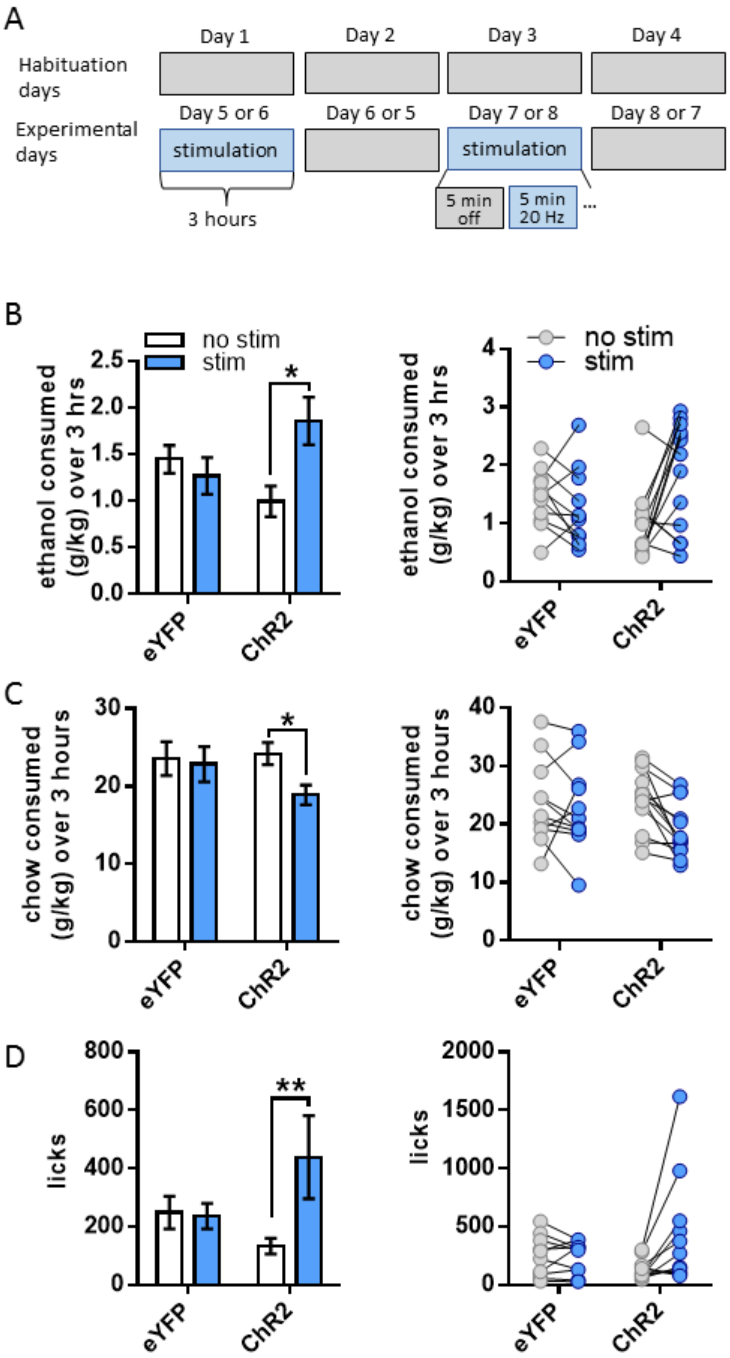

Figure 4– *NTS*$^{CeA→PBN}$::ChR2-eYFP stimulation increases ethanol consumption and reduces food consumption (a) *NTS*^{CeAàPBN}::ChR2 mice (n=13) consumed more 6% ethanol on stimulation days, whereas *NTS*^{CeAàPBN}::eYFP mice (n=11) showed no effect of stimulation. (Wilcoxon matched-pairs signed rank test: control W=-20, p=0.4131; ChR2 W=61, p=0.0327). (b) *NTS*^{CeAàPBN}::ChR2 mice (n=11) also showed increased licks to the ethanol bottle during the 5 minute stimulation epochs. *NTS*^{CeAàPBN}::eYFP mice (n=10) were again unaffected. (Wilcoxon matched-pairs signed rank test: control W=-20, p=0.4131; ChR2 W=61, p=0.0327). (c) Stimulation also induced the *NTS*^{CeAàPBN}::ChR2 mice (n=13) to consume less chow on stimulation days. Again, *NTS*^{CeAàPBN}::eYFP mice (n=11) showed no change. (Two-way ANOVA: interaction $F_{(1,22)}$=4.313, p=0.0497; virus type, $F_{(1,22)}$=0.5391, p=0.4705; stimulation, $F_{(1,22)}$= 7.387, p=0.0126). Paired t-test **p<0.01).

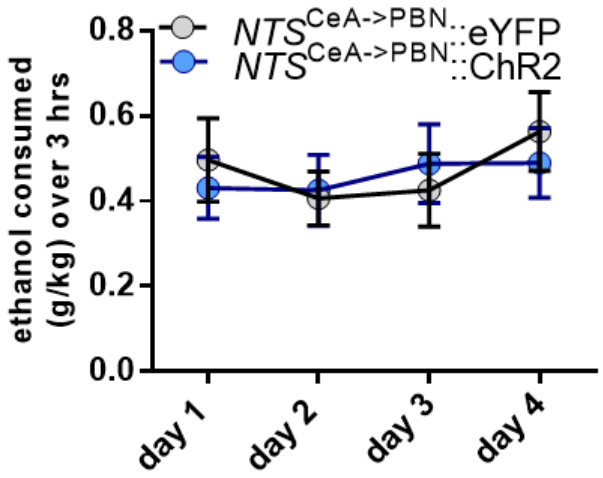

Supplementary Figure 7- Phenotyper Ethanol consumption habituation *NTS*^{CeAàPBN}::ChR2 (n=14) and *NTS*^{CeAàPBN}::eYFP (n=11) mice did not show differences in ethanol drinking during habituation days. (Two-way ANOVA: interaction, $F_{(3,66)}$=0.5483, p=0.6510; day, $F_{(3,66)}$=1.054, p=0.3746; virus type $F_{(1,22)}$=0.02512, p=0.8755).

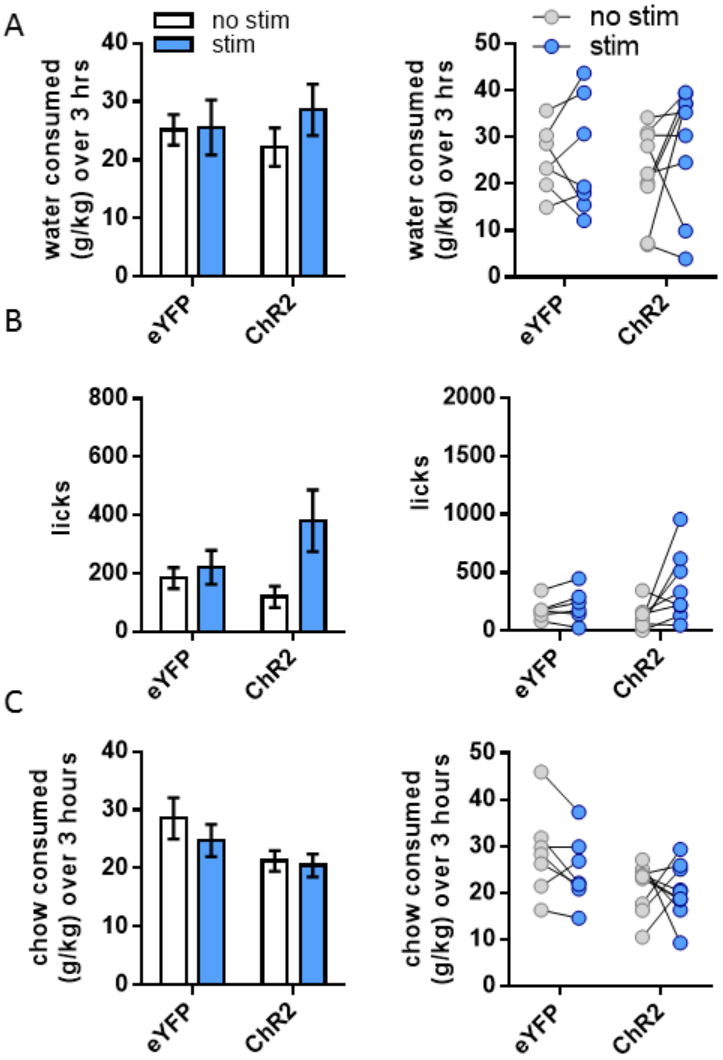

Figure 5 – *NTS*$^{CeA→PBN}$::ChR2-eYFP stimulation does not alter water consumption or food consumption in the presence of water (a) *NTS*^{CeAàPBN}::ChR2 (n=7) and *NTS*^{CeAàPBN}::eYFP (n=9) mice did not show changes in water drinking following stimulation. (Two-way ANOVA: interaction $F_{(1,14)}$=0.9252, p=0.3524; virus type, $F_{(1,14)}$=9.541e-005, p=0.9923; stimulation, $F_{(1,14)}$=1.203, p=0.2913). (b) *NTS*^{CeAàPBN}::ChR2 (n=8) and *NTS*^{CeAàPBN}::eYFP (n=6) mice did not alter licking to the water bottle during stimulation. (Wilcoxon matched-pairs signed rank test: control W=13, p=0.2188; ChR2 W=26, p=0.0781).(c) *NTS*^{CeAàPBN}::ChR2 (n=7) and *NTS*^{CeAàPBN}::eYFP (n=9) mice did not show changes in food consumption. (Two-way ANOVA: interaction $F_{(1,14)}$=0.5311, p=0.4782; virus type, $F_{(1,14)}$=4.257, p=0.0581; stimulation, $F_{(1,14)}$=1.218, p=0.2883).

References

Anderson RI, Becker HC (2017). Role of the Dynorphin/Kappa Opioid Receptor System in the Motivational Effects of Ethanol. *Alcohol Clin Exp Res* **41**: 1402–1418.

Betley JN, Xu S, Cao ZFH, Gong R, Magnus CJ, Yu Y, *et al* (2015). Neurons for hunger and thirst transmit a negative-valence teaching signal. *Nature* **521**: 180–185.

Binder EB, Kinkead B, Owens MJ, Nemeroff CB (2001). Neurotensin and Dopamine Interactions. *Pharmacol Rev* **53**: 453.

Cáceda R, Kinkead B, Nemeroff CB (2006). Neurotensin: Role in psychiatric and neurological diseases. *Peptides* **27**: 2385–2404.

Cai H, Haubensak W, Anthony TE, Anderson DJ (2014). Central amygdala PKC-δ+ neurons mediate the influence of multiple anorexigenic signals. *Nat Neurosci* **17**: 1240–1248.

Carter ME, Han S, Palmiter RD (2015). Parabrachial Calcitonin Gene-Related Peptide Neurons Mediate Conditioned Taste Aversion. *J Neurosci* **35**: 4582–4586.

Carter ME, Soden ME, Zweifel LS, Palmiter RD (2013). Genetic identification of a neural circuit that suppresses appetite. *Nature* **503**: 111–114.

Chang SL, Patel NA, Romero AA (1995). Activation and desensitization of Fos immunoreactivity in the rat brain following ethanol administration. *Brain Res* **679**: 89–98.

Chavkin C, James I, Goldstein A (1982). Dynorphin is a specific endogenous ligand of the kappa opioid receptor. *Science* **215**: 413–415.

Douglass AM, Kucukdereli H, Ponserre M, Markovic M, Gründemann J, Strobel C, *et al* (2017). Central Amygdala Circuits Modulate Food Consumption Through A Positive Valence Mechanism. doi:10.1101/145375.

Fitzpatrick K, Winrow CJ, Gotter AL, Millstein J, Arbuzova J, Brunner J, *et al* (2012). Altered Sleep and Affect in the Neurotensin Receptor 1 Knockout Mouse. *Sleep* **35**: 949–956.

Gilpin NW, Herman MA, Roberto M (2015). The Central Amygdala as an Integrative Hub for Anxiety and Alcohol Use Disorders. *Biol Psychiatry* **77**: 859–869.

Grigson PS, Reilly S, Shimura T, Norgren R (1998). Ibotenic acid lesions of the parabrachial nucleus and conditioned taste aversion: Further evidence for an associative deficit in rats. *Behav Neurosci* **112**: 160–171.

Guglielmo G de, Crawford E, Kim S, Vendruscolo LF, Hope BT, Brennan M, *et al* (2016). Recruitment of a Neuronal Ensemble in the Central Nucleus of the Amygdala Is Required for Alcohol Dependence. *J Neurosci* **36**: 9446–9453.

Haubensak W, Kunwar PS, Cai H, Ciocchi S, Wall NR, Ponnusamy R, *et al* (2010). Genetic dissection of an amygdala microcircuit that gates conditioned fear. *Nature* **468**: 270–276.

Herman MA, Contet C, Justice NJ, Vale W, Roberto M (2013). Novel Subunit-Specific Tonic GABA Currents and Differential Effects of Ethanol in the Central Amygdala of CRF Receptor-1 Reporter Mice. *J Neurosci* **33**: 3284–3298.

Hwa LS, Chu A, Levinson SA, Kayyali TM, DeBold JF, Miczek KA (2011). Persistent Escalation of Alcohol Drinking in C57BL/6J Mice With Intermittent Access to 20% Ethanol: ESCALATED ALCOHOL AFTER INTERMITTENT ACCESS. *Alcohol Clin Exp Res* **35**: 1938–1947.

Hyytiä P, Koob GF (1995). GABAA receptor antagonism in the extended amygdala decreases ethanol self-administration in rats. *Eur J Pharmacol* **283**: 151–159.

Jennings JH, Rizzi G, Stamatakis AM, Ung RL, Stuber GD (2013a). The Inhibitory Circuit Architecture of the Lateral Hypothalamus Orchestrates Feeding. *Science* **341**: 1517–1521.

Jennings JH, Sparta DR, Stamatakis AM, Ung RL, Pleil KE, Kash TL, *et al* (2013b). Distinct extended amygdala circuits for divergent motivational states. *Nature* **496**: 224–228.

Kempadoo KA, Tourino C, Cho SL, Magnani F, Leinninger G-M, Stuber GD, *et al* (2013). Hypothalamic Neurotensin Projections Promote Reward by Enhancing Glutamate Transmission in the VTA. *J Neurosci* **33**: 7618–7626.

Kim J, Zhang X, Muralidhar S, LeBlanc SA, Tonegawa S (2017). Basolateral to Central Amygdala Neural Circuits for Appetitive Behaviors. *Neuron* **93**: 1464–1479.e5.

Koob GF (2015). The dark side of emotion: The addiction perspective. *Eur J Pharmacol* **753**: 73–87.

Koob GF, Buck CL, Cohen A, Edwards S, Park PE, Schlosburg JE, *et al* (2014). Addiction as a stress surfeit disorder. *Neuropharmacology* **76**: 370–382.

Koob GF, Sanna PP, Bloom FE (1998). Neuroscience of Addiction. *Neuron* **21**: 467–476.

Lee MR, Hinton DJ, Song JY, Lee KW, Choo C, Johng H, *et al* (2010). Neurotensin receptor type 1 regulates ethanol intoxication and consumption in mice. *Pharmacol Biochem Behav* **95**: 235–241.

Lee MR, Hinton DJ, Unal SS, Richelson E, Choi D-S (2011). Increased Ethanol Consumption and Preference in Mice Lacking Neurotensin Receptor Type 2: NEUROTENSIN RECEPTOR TYPE 2 AND ALCOHOLISM. *Alcohol Clin Exp Res* **35**: 99–107.

Leinninger GM, Opland DM, Jo Y-H, Faouzi M, Christensen L, Cappellucci LA, *et al* (2011). Leptin Action via Neurotensin Neurons Controls Orexin, the Mesolimbic Dopamine System and Energy Balance. *Cell Metab* **14**: 313–323.

Lowery-Gionta EG, Navarro M, Li C, Pleil KE, Rinker JA, Cox BR, *et al* (2012). Corticotropin Releasing Factor Signaling in the Central Amygdala is Recruited during Binge-Like Ethanol Consumption in C57BL/6J Mice. *J Neurosci* **32**: 3405–3413.

Mahler SV, Berridge KC (2009). Which Cue to "Want?" Central Amygdala Opioid Activation Enhances and Focuses Incentive Salience on a Prepotent Reward Cue. *J Neurosci* **29**: 6500–6513.

McCall JG, Al-Hasani R, Siuda ER, Hong DY, Norris AJ, Ford CP, *et al* (2015). CRH Engagement of the Locus Coeruleus Noradrenergic System Mediates Stress-Induced Anxiety. *Neuron* **87**: 605–620.

McHenry JA, Otis JM, Rossi MA, Robinson JE, Kosyk O, Miller NW, *et al* (2017). Hormonal gain control of a medial preoptic area social reward circuit. *Nat Neurosci* **20**: 449–458.

Moga MM, Gray TS (1985). Evidence for corticotropin-releasing factor, neurotensin, and somatostatin in the neural pathway from the central nucleus of the amygdala to the parabrachial nucleus. *J Comp Neurol* **241**: 275–284.

Möller C, Wiklund L, Sommer W, Thorsell A, Heilig M (1997). Decreased experimental anxiety and voluntary ethanol consumption in rats following central but not basolateral amygdala lesions. *Brain Res* **760**: 94–101.

Morgan CW, Julien O, Unger EK, Shah NM, Wells JA (2014). Turning ON Caspases with Genetics and Small Molecules. *Methods Enzymol* **544**: 179–213.

Pleil KE, Rinker JA, Lowery-Gionta EG, Mazzone CM, McCall NM, Kendra AM, *et al* (2015). NPY signaling inhibits extended amygdala CRF neurons to suppress binge alcohol drinking. *Nat Neurosci* **18**: 545–552.

Prus AJ, Hillhouse TM, LaCrosse AL (2014). Acute, but not repeated, administration of the neurotensin NTS1 receptor agonist PD149163 decreases conditioned footshock-induced ultrasonic vocalizations in rats. *Prog Neuropsychopharmacol Biol Psychiatry* **49**: 78–84.

Roberto M, Madamba SG, Stouffer DG, Parsons LH, Siggins GR (2004). Increased GABA Release in the Central Amygdala of Ethanol-Dependent Rats. *J Neurosci* **24**: 10159–10166.

Robinson MJF, Warlow SM, Berridge KC (2014). Optogenetic Excitation of Central Amygdala Amplifies and Narrows Incentive Motivation to Pursue One Reward Above Another. *J Neurosci* **34**: 16567–16580.

Ryan PJ, Ross SI, Campos CA, Derkach VA, Palmiter RD (2017). Oxytocin-receptor-expressing neurons in the parabrachial nucleus regulate fluid intake. *Nat Neurosci* **20**: 1722–1733.

Sparta DR, Stamatakis AM, Phillips JL, Hovelsø N, Zessen R van, Stuber GD (2011). Construction of implantable optical fibers for long-term optogenetic manipulation of neural circuits. *Nat Protoc* **7**: 12–23.

Swanson LW (1976). The locus coeruleus: A cytoarchitectonic, golgi and immunohistochemical study in the albino rat. *Brain Res* **110**: 39–56.

Thiele TE, Roitman MF, Bernstein llene L (1996). c-Fos Induction in Rat Brainstem in Response to Ethanol- and Lithium Chloride-Induced Conditioned Taste Aversions. *Alcohol Clin Exp Res* **20**: 1023–1028.

Tye KM, Prakash R, Kim S-Y, Fenno LE, Grosenick L, Zarabi H, *et al* (2011). Amygdala circuitry mediating reversible and bidirectional control of anxiety. *Nature* **471**: 358–362.

Warlow SM, Robinson MJF, Berridge KC (2017). Optogenetic central amygdala stimulation intensifies and narrows motivation for cocaine. *J Neurosci* 3141–16doi:10.1523/JNEUROSCI.3141-16.2017.

Yang CF, Chiang MC, Gray DC, Prabhakaran M, Alvarado M, Juntti SA, *et al* (2013). Sexually Dimorphic Neurons in the Ventromedial Hypothalamus Govern Mating in Both Sexes and Aggression in Males. *Cell* **153**: 896–909.